Rate and equilibrium constant measurements for gas-phase proton-transfer reactions involving H_2O, H_2S, HCN, and H_2CO

KENICHIRO TANAKA,[1] GERVASE I. MACKAY, AND DIETHARD K. BOHME[2]

Department of Chemistry and Centre for Research in Experimental Space Science, York University, Downsview, Ont., Canada M3J 1P3

Received July 15, 1977

KENICHIRO TANAKA, GERVASE I. MACKAY, and DIETHARD K. BOHME. Can. J. Chem. **56**, 193 (1978).

The flowing afterglow technique has been employed in the measurement of rate and equilibrium constants at 296 ± 2 K for unsolvated proton transfer reactions of the type $XH^+ + Y \leftrightarrows YH^+ + X$ and several solvated proton transfer reactions of the type $XH^+{\cdot}X + Y \leftrightarrows YH^+{\cdot}X + Y$ where X and Y may be H_2O, H_2S, HCN, or H_2CO. Where possible, direct comparisons are made with similar measurements performed with other techniques. The equilibrium constant measurements provide a measure of the relative proton affinities of H_2O, H_2S, HCN, and H_2CO and absolute values for $PA(H_2O) = 166.4 \pm 2.4$ kcal mol^{-1}, $PA(H_2S) = 170.2 \pm 1.8$ kcal mol^{-1}, and $PA(HCN) = 171.0 \pm 1.7$ kcal mol^{-1} when reference is made to $PA(H_2CO) = 170.9 \pm 1.2$ kcal mol^{-1} which can be derived from available thermochemical information. The rate constant measurements reinforce the generalization that unsolvated proton transfer involving simple molecules proceeds with high efficiency and provide information about the influence of solvation on this efficiency.

KENICHIRO TANAKA, GERVASE I. MACKAY et DIETHARD K. BOHME. Can. J. Chem. **56**, 193 (1978).

On a utilisé la technique d'écoulement post-luminescent dans le but de mesurer les constantes de vitesse et d'équilibre à 296 ± 2 K des réactions de transfert de protons non-solvatés du type $XH^+ + Y \leftrightarrows YH^+ + X$ et pour plusieurs réactions de transfert de protons solvatés du type $XH^+{\cdot}X + Y \leftrightarrows YH^+{\cdot}X + Y$ où X et Y peuvent être H_2O, H_2S, HCN ou H_2CO. Lorsque la possibilité existait, on a fait des comparaisons directes avec des mesures semblables effectuées par d'autres techniques. Les mesures de constante d'équilibre nous ont fourni une mesure des affinités relatives des protons pour H_2O, H_2S, HCN et H_2CO et des valeurs absolues pour $PA(H_2O) = 166.4 \pm 2.4$ kcal mol^{-1}, $PA(H_2S) = 170.2 \pm 1.8$ kcal mol^{-1} et $PA(HCN) = 171.0 \pm 1.7$ kcal mol^{-1} lorsque l'on se réfère à une valeur de $PA(H_2CO) = 170.9 \pm 1.2$ kcal mol^{-1} qui peut être obtenue à partir de données thermochimiques. Les mesures de constantes de vitesse renforcent la généralisation à l'effet que le transfert d'un proton non-solvaté impliquant des molécules simples se produit avec une grande efficacité et fournissent une information concernant l'influence de la solvatation sur cette efficacité.

[Traduit par le journal]

Introduction

Over the past few years a variety of gas-phase experimental techniques have been applied to the determination of the relative proton affinities of molecules through measurements which attempt to establish values for equilibrium constants of proton-transfer reactions of the type

$$XH^+ + Y \rightleftarrows YH^+ + X \quad [1]$$

proceeding in partially ionized gas mixtures at both low and high total pressures (1). Such measurements have led to reports of relative proton affinity 'ladders' incorporating a large number and variety of inorganic and organic molecules. Absolute scales are assigned to such ladders usually with the aid of thermodynamic information gained from (nonequilibrium) photon or electron impact studies.

The purpose of this study is twofold. It is directed in part towards a determination of the absolute proton affinities of HCN, H_2S, and H_2O. Equilibrium constant measurements are attempted for reactions of type [1] which allow the construction of a relative proton affinity ladder which links these molecules to H_2CO. Absolute values for proton affinities are derived to within ±2 kcal mol^{-1} by referring to the proton affinity of H_2CO which can be established from the photoionization appearance potential measurements of H_2COH^+ from CH_3OH reported by Refaey and Chupka (2). Such an accuracy is acceptable for most chemical applications. The proton affinity of H_2O is, of course, of special importance and interest. Unfortunately, its value has experienced a considerable variation with time. Only very recently, equilibrium constant measurements made

---

[1] Present address: Institute for Molecular Science, Myodaiji, Okazaki, Aichi, Japan.

[2] Alfred P. Sloan Research Fellow, 1974–1976.

with a high-pressure pulsed electron-beam ion source mass spectrometer (3) and with low-pressure pulsed ion cyclotron resonance (4) have suggested values for $PA_{298}(H_2O) = 169 \pm 2$ and 170 ± 2 kcal mol^{-1}, respectively, which are somewhat higher than the value of 165 ± 3 kcal mol^{-1} previously preferred by Long and Munson (5).

Secondly, the equilibrium constant measurements chosen in this study allow direct comparisons to be made with similar measurements performed with other techniques which employ a variety of modes of ion production, containment, and detection and encompass a wide range of operating conditions such as total pressure, ion and neutral concentrations, temperature, reaction time, and ambient electric fields. Such comparisons, which have not been as frequent as one might have expected, are instructive in establishing the applicability and reliability of the various techniques which have been employed for such measurements (6–8).

Experimental

The experiments were performed with a flowing afterglow system in the manner described previously (9). The reactant ions $XH^+ = H_3O^+$, H_3S^+, H_2CN^+, and H_2COH^+ were established in a flowing hydrogen plasma by fast proton-transfer reactions of the type

$$[2] \qquad H_3^+ + X \rightarrow XH^+ + H_2$$

which proceed upon the addition of the appropriate gas X downstream of the ionizer. H_3^+ was established by the fast reaction

$$[3] \qquad H_2^+ + H_2 \rightarrow H_3^+ + H$$

Sufficient X was added to ensure that reaction 2 reached completion prior to the reaction region. H_3O^+ was also generated in a helium–water vapour plasma by the reaction

$$[4] \qquad H_2O^+ + H_2O \rightarrow H_3O^+ + OH$$

The neutral reactants were added sufficiently downstream of the ion production region to ensure thermalization of the XH^+ ions by collisions with the carrier gas molecules to the ambient temperature of 296 ± 2 K prior to reaction. The total pressure in the reaction region was in the range $P = 0.27$ to 0.65 Torr, the effective reaction length had values in the range $L = 59$–85 cm, and the average flow velocity had values in the range $\bar{v} = 7.3$–8.2×10^3 cm s^{-1}. At the end of the reaction region the plasma was sampled with a quadrupole mass spectrometer through a small orifice mounted at the tip of a sampling nose cone. The observed variations in the reactant and product ion signals as a function of reactant gas addition at a fixed addition of the back-reactant gas provided the raw data from which the rate and equilibrium constants were derived.

The gases used were helium (Linde, Prepurified Grade, 99.995% He), hydrogen (Linde, Very Dry Grade, 99.95% H_2), and H_2S (Matheson, C.P. Grade, 99.5% H_2S). The water vapour was derived from either boiled tap water or boiled distilled water. The HCN was prepared by the action of sulfuric acid on an aqueous solution of KCN (10), dried by passing over anhydrous $CaCl_2$, and further purified by distillation *in vacuo*. Monomeric formaldehyde was prepared from paraformaldehyde (Fisher Scientific, Purified Grade) by an adaptation of the method developed by Spence and Wild (11). Paraformaldehyde was distilled at low pressures at ~370 K. The formaldehyde was then dried by passing it through a cold trap at 195 K and frozen out at liquid nitrogen temperatures. A gaseous mixture of ~5% formaldehyde in helium was used in these studies. The partial pressure of the formaldehyde was maintained at between 5 and 7 Torr to avoid polymerization. The monomer could be stored at these pressures for several days with negligible polymerization.

All experiments were carried out at a room temperature of 296 ± 2 K.

Results

The results of the measurements of rate and equilibrium constants for the proton-transfer reactions investigated in this study are summarized in Tables 1 and 2. An account of the data analysis and sources of error has been given previously (9, 14). Complications which may arise as a result of diffusion, competing reaction channels, and clustering reactions of the reactant and product ions have also been dealt with in detail elsewhere (14, 15).

Reaction 5

$$[5] \qquad H_3O^+ + H_2S \rightleftharpoons H_3S^+ + H_2O$$

The reaction of H_3O^+ with H_2S was observed to proceed rapidly by proton transfer to produce H_3S^+. Equilibrium was achieved in both H_2 (eight experiments) and He (five experiments) carrier gases over a range of $P = 0.290$–0.65 Torr and flow of H_2O from 2.13 to 4.96×10^{18} molecules s^{-1}. There was no evidence for the occurrence of competing reaction channels and no serious complications were introduced into the data analysis under these conditions by the clustering reactions of H_3O^+ with H_2O and H_3S^+ with H_2S. Figure 1 illustrates the determination of k_5, k_{-5} and k_5/k_{-5} from a fit to the H_3O^+ decay, whereas Fig. 2 indicates the determination of K_5 from the variation of the product to reactant ion signal ratio (corrected for mass discrimination) with H_2S addition. The cluster ions $H_3O^+{\cdot}H_2O$ and $H_3O^+{\cdot}2H_2O$ did not react rapidly with H_2S, $k \lesssim 10^{-12}$ cm^3 $molecule^{-1}$ s^{-1}. Their initial decay shown in Fig. 1 is due to the depletion in the reaction region of the precursor ions, H_3O^+ and $H_3O^+{\cdot}H_2O$, respectively.

Trace amounts of SF_6 were added in one H_2 and one He experiment to test the validity of the assumption of equal diffusion losses for H_3O^+ and H_3S^+. The values derived for k_5/k_{-5} (from the fit to the H_3O^+ decay) and K_5 (from the ratio plot) were observed to be insensitive to the change in the mode of diffusion from ion–electron to ion–ion brought about by the added SF_6.

Reaction 6

[6] $H_3O^+ + HCN \rightleftharpoons H_2CN^+ + H_2O$

H_3O^+ was observed to react rapidly with HCN to produce H_2CN^+ in four experiments in which H_2 was used as the carrier gas. Equilibrium was achieved in all four experiments over a range of P = 0.342–0.405 Torr and a range of H_2O flow from 3.61 to 4.59×10^{18} molecules s^{-1}. Again there was no evidence for the occurrence of competing reaction channels and no serious complications were introduced into the data analysis by the occurrence of clustering reactions. $H_3O^+{\cdot}H_2O$ appeared to react with HCN, $k = 1 \times 10^{-10}$ cm^3 $molecule^{-1}$ s^{-1}. A concomitant increase in the $m/e = 46$ signal suggested the occurrence of what might, in this context, be more appropriately regarded as a solvated proton-transfer reaction:

[7] $H_3O^+{\cdot}H_2O + HCN \rightarrow H_2CN^+{\cdot}H_2O + H_2O$

rather than a solvent 'switching' reaction:

[8] $H_3O^+{\cdot}H_2O + HCN \rightarrow H_3O^+{\cdot}HCN + H_2O$

The analysis of the behaviour of the $H_3O^+{\cdot}2H_2O$ signal was complicated by its overlap at $m/e = 55$ with $H_2CN^+{\cdot}HCN$.

Reaction 9

[9] $H_3S^+ + HCN \rightleftharpoons H_2CN^+ + H_2S$

The equilibrium for this reaction was approached from both directions in H_2 carrier gas. Seven experiments were carried out in the forward direction over a range of P = 0.362–0.51 Torr and flow of H_2S from 0.247 to 3.24×10^{18} molecules s^{-1}. Proton transfer was the only observed reaction channel. Equilibrium was achieved in six experiments. The product H_2CN^+ was observed to react further at large additions of HCN to produce the cluster ion $H_2CN^+{\cdot}HCN$. Our standard analysis (9) allowed a good fit to the H_3S^+ decay and the H_2CN^+/H_3S^+ ion signal ratio plot at additions of HCN below $\sim 1 \times 10^{18}$ molecule s^{-1}. At higher additions the rate of the reaction of H_2CN^+ with HCN appeared to approach that for the back reaction of H_2CN^+ with H_2S to an extent sufficient to drive the reaction slightly out of equilibrium (case 5 in ref. 14).

The perturbation introduced by the further reaction of the product ion with the added reactant gas apparent in the attainment of equilibrium in the forward direction was observed to be less severe in the reverse direction presumably as a result of the lower rate of association of H_3S^+ with H_2S. Five experiments were carried out in the reverse direction in H_2 carrier gas at pressures P = 0.363–0.61 Torr

TABLE 1. Summary of the measured values of k_f/k_r and K at 296 ± 2 K together with estimates of their accuracies

	k_f/k_r[a]				K[b]			
Reaction	N[c]	Forward	N	Reverse	N	Forward	N	Reverse
$H_3O^+ + H_2S \rightleftharpoons H_3S^+ + H_2O$	13	$(5.5 \pm 1.7) \times 10^2$			13	$(6.2 \pm 2.2) \times 10^2$		
$H_3O^+ + HCN \rightleftharpoons H_2CN^+ + H_2O$	4	$(4.1 \pm 1.2) \times 10^3$			4	$(3.8 \pm 1.3) \times 10^3$		
$H_3S^+ + HCN \rightleftharpoons H_2CN^+ + H_2S$	7	5.6 ± 1.4	5	4.8 ± 1.0	6	5.7 ± 1.4	5	4.8 ± 1.0
$H_3S^+ + H_2CO \rightleftharpoons H_2COH^+ + H_2S$	4	≤ 13	4	≥ 9.3	4	11.3 ± 4.5	4	9.2 ± 3.7
$H_2CN^+ + H_2CO \rightleftharpoons H_2COH^+ + HCN$	1	<4	3	1.9 ± 0.7	2	1.6 ± 0.6	3	1.4 ± 0.5
$H_2CN^+{\cdot}HCN + H_2CO \rightleftharpoons H_2COH^+{\cdot}HCN + HCN$	1	8.9 ± 2.2			1	8.8 ± 2.2	3	8.6 ± 3.0
$H_2COH^+{\cdot}H_2CO + HCN \rightleftharpoons H_2CN^+{\cdot}H_2CO + H_2CO$					3	1.6 ± 0.6		

[a] Determined from a fit to the decay of the reactant ion (analysis B ref. 9) with a precision ≲ 20%.
[b] Determined from the slope of the ratio plot and corrected for mass discrimination (analysis C ref. 9) with a precision ≲ 20%.
[c] N represents the number of measurements.

TABLE 2. Summary of the experimental measurements of rate constants (10^{-9} cm^3 molecule^{-1} s^{-1}) and equilibrium constants at 296 ± 2 K

Reaction	k_{forward}[a]	N[b]	K[c]	N
$H_3O^+ + H_2S \rightleftharpoons H_3S^+ + H_2O$	1.9 ± 0.1	13	$(5.8 \pm 1.3) \times 10^2$	26
$H_3O^+ + HCN \rightleftharpoons H_2CN^+ + H_2O$	3.5 ± 0.3	11[d]	$(4.0 \pm 0.9) \times 10^3$	8
$H_3S^+ + HCN \rightleftharpoons H_2CN^+ + H_2S$	1.5 ± 0.1	7	5.1 ± 0.6	23
$H_3S^+ + H_2CO \rightleftharpoons H_2COH^+ + H_2S$	2.2 ± 0.1	3	10.0 ± 2.9	8
$H_2CN^+ + H_2CO \rightleftharpoons H_2COH^+ + HCN$	>1.6		1.6 ± 0.3	8
$H_2CN^+ \cdot HCN + H_2CO \rightleftharpoons H_2COH^+ \cdot HCN + HCN$	0.60	1	8.8 ± 1.8	5
$H_2COH^+ \cdot H_2CO + HCN \rightleftharpoons H_2CN^+ \cdot H_2CO + H_2CO$	$\gtrsim 0.1$		1.6 ± 0.6	3
$H_3O^+ \cdot H_2O + H_2S \rightarrow H_3S^+ \cdot H_2O + H_2O$	$\lesssim 0.001$			
$H_3O^+ \cdot 2H_2O + H_2S \rightarrow H_3S^+ \cdot 2H_2O + H_2O$	$\lesssim 0.001$			
$H_3O^+ \cdot H_2O + HCN \rightarrow H_2CN^+ \cdot H_2O + H_2O$	0.10	2		
$H_2CN^+ \cdot HCN + H_2S \rightarrow H_3S^+ \cdot HCN + HCN$	$\lesssim 0.001$			

[a] Values for k_{forward} were determined using either analysis A or B (9). The limits given along with the mean value represent the precision. The accuracy is estimated to be ±20% for the reactions of H_3O^+, ±25% for the reactions of H_3S^+, and ±30% for the reactions of $H_2CN^+ \cdot HCN$ and $H_3O^+ \cdot H_2O$.

[b] N represents the number of measurements.

[c] The value of K represents the weighted mean together with the standard error of measurements of k_f/k_r and K in one or both directions of the reaction (12).

[d] Includes seven previous determinations (13).

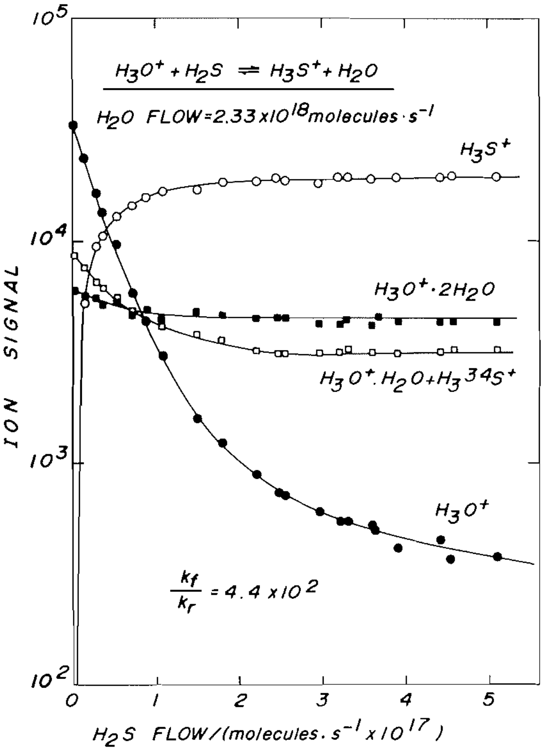

FIG. 1. The observed variation of H_3O^+, $H_3O^+ \cdot H_2O$, and $H_3O^+ \cdot 2H_2O$ upon the addition of H_2S into a H_2O–H_2 plasma in which H_3O^+ is initially a dominant ion. The solid line drawn through the H_3O^+ decay is a fit which provides the values $k_f = 1.9 \times 10^{-9}$ cm^3 molecule^{-1} s^{-1}, $k_r = 4.4 \times 10^{-12}$ cm^3 molecule^{-1} s^{-1}, and $k_f/k_r = 4.4 \times 10^2$ for the proton transfer to H_2S; T = 296 K, P = 0.432 Torr, $\bar{v}$ = 7.7 × 10^3 cm s^{-1}, and L = 85 cm.

and HCN flows in the range from 0.92 to 3.05 × 10^{17} molecules s^{-1}. The equilibrium constant derived from fits to the observed H_2CN^+ decays and the H_3S^+/H_2CN^+ ion signal ratio plots corrected for mass discrimination was in good agreement with that determined from the study of the forward direction. The $H_2CN^+ \cdot HCN$ present in the reaction region was observed not to react rapidly with the added H_2S, $k \lesssim 10^{-12}$ cm^3 molecule^{-1} s^{-1}.

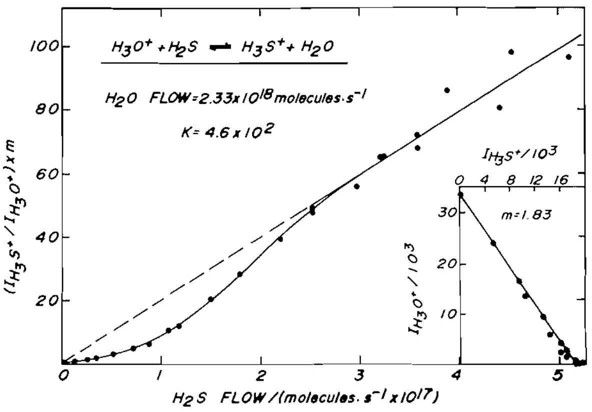

FIG. 2. The observed variation of the product to reactant ion signal ratio (corrected for mass discrimination) with the flow of neutral reactant, H_2S, at constant flow of neutral back reactant, H_2O. The initial curvature reflects the approach to equilibrium. The insert illustrates the determination of the mass discrimination factor, m; T = 296 K, P = 0.432 Torr, $\bar{v}$ = 7.7 × 10^3 cm s^{-1}, and L = 85 cm.

Reaction 10

[10] $H_3S^+ + H_2CO \rightleftharpoons H_2COH^+ + H_2S$

This reaction was also investigated in both directions in H_2 carrier gas. Four experiments were carried out in the forward direction over a range of P = 0.268–0.336 Torr and flow of H_2S from 2.04 to 9.6 × 10^{17} molecules s^{-1}. The results for one of these experiments is shown in Fig. 3 which indicates the production of H_2COH^+ from H_3S^+ as H_2CO is added into the flowing plasma. H_2COH^+ appears to react further with H_2CO to form the cluster ion $H_2COH^+{\cdot}H_2CO$ presumably via a three-body association reaction. The production of CH_3S^+, which was observed to be enhanced at the higher flows of H_2S, can be attributed to reaction 11 which is exothermic by several kcal mol^{-1}.

$$[11] \qquad H_2COH^+ + H_2S \rightarrow CH_3S^+ + H_2O$$

Both reaction 11 and the association reaction of H_2COH^+ with H_2CO act as sinks for H_2COH^+ which compete with the reverse proton transfer [−10] and can prevent the establishment of true equilibrium. The incorporation of reasonable rates for these reactions into an extended analysis (case 2 and case 5 in ref. 14) indicated that the decay of H_3S^+ shows decreased curvature under these conditions so that the apparent value of k_{10}/k_{-10} determined from a fit to the H_3S^+ decay should be regarded as an upper limit to the true value. However the apparent value of the equilibrium constant determined from the ratio plot should still be nearly equal to the true value under these same conditions.

Four experiments were carried out in which H_2S was added into a flowing H_2 plasma in which H_2COH^+ was initially the dominant ion. Values of P were in the range 0.296–0.339 Torr and the flow of H_2CO had values in the range 0.71–1.95 × 10^{17} molecules s^{-1}. The proton-transfer reaction −10 was again observed to proceed in competion with reaction 11. Neither H_3S^+ nor CH_3S^+ appeared to react further with H_2S, $k \lesssim 10^{-12}$ cm^3 molecule^{-1} s^{-1}. The H_3S^+/CH_3S^+ ion signal ratio at saturation which was observed to be independent of H_2CO addition led to a value for $k_{-10}/k_{11} \cong 5$. In this case the extended analysis (case 4 in ref. 14) indicated that the apparent value of k_{-10}/k_{10} determined from a fit to the H_2COH^+ decay should be regarded as an upper limit to the true value and hence a lower limit to the true value of k_{10}/k_{-10}. However, the ratio plot should again provide a good measure of the true equilibrium constant.

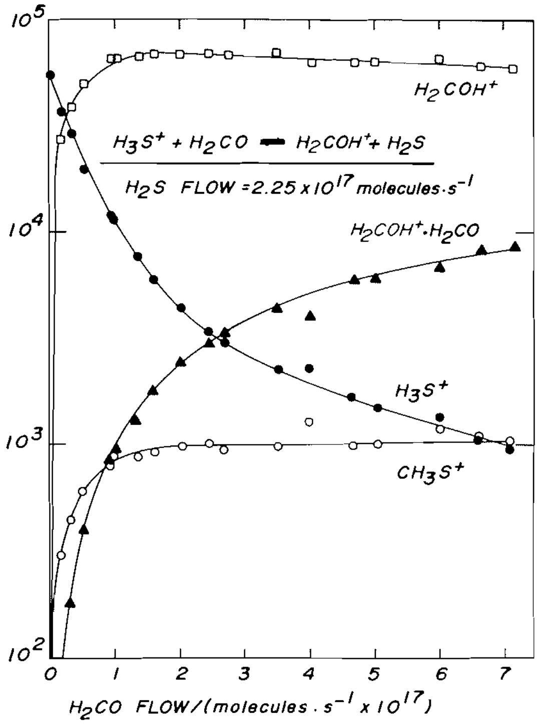

FIG. 3. The observed variation of ion signals with the flow of H_2CO at constant flow of H_2S. The solid line drawn through the H_3S^+ decay is a fit which provides values for $k_f = 2.1 \times 10^{-9}$ cm^3 molecule^{-1} s^{-1} and $k_f/k_r \leq 15$; $T = 297$ K, $P = 0.308$ Torr, $\bar{v} = 7.5 \times 10^3$ cm s^{-1}, and $L = 59$ cm.

Reaction 12

$$[12] \qquad H_2CN^+ + H_2CO \rightleftharpoons H_2COH^+ + HCN$$

The interconversion of ions observed upon the addition of H_2CO into a flowing HCN–H_2 plasma in which H_2CN^+ is initially a dominant ion is illustrated in Fig. 4. H_2CN^+ appeared to react with H_2CO by proton transfer only to produce H_2COH^+ which reacted further with H_2CO to form the

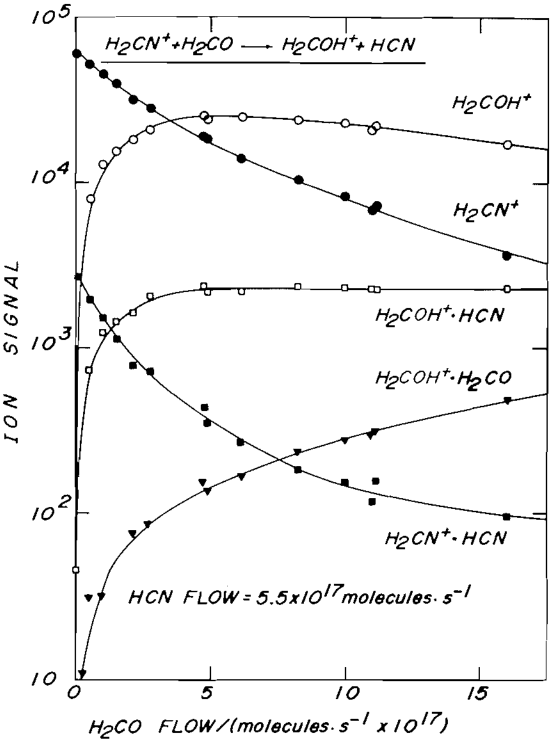

FIG. 4. The observed variation of ion signals with the flow of H_2CO at constant flow of HCN. The solid line drawn through the H_2CN^+ decay is a fit which provides values for $k_f \geq 1.6 \times 10^{-9}$ cm^3 molecule^{-1} s^{-1} and $k_f/k_r < 4$; $T = 297$ K, $P = 0.371$ Torr, $\bar{v} = 8.1 \times 10^3$ cm s^{-1}, and $L = 85$ cm.

$H_2COH^+ \cdot H_2CO$ cluster ion. The rate of this latter reaction was sufficient to allow the determination of only a reliable upper limit to k_{12}/k_{-12} (case 5 in ref. 14) from a fit to the H_2CN^+ decay while the corresponding ratio plot still allowed a reasonable measure of K_{12}.

It is also apparent from Fig. 4 that $H_2CN^+ \cdot HCN$ reacts with H_2CO in a manner which may be represented by the solvated proton-transfer reaction

[13] $H_2CN^+ \cdot HCN + H_2CO \rightarrow H_2COH^+ \cdot HCN + HCN$

The decay of the $H_2CN^+ \cdot HCN$ signal and the $H_2COH^+ \cdot HCN/H_2CN^+ \cdot HCN$ ratio plot provided values for $k_{13} = (6 \pm 2) \times 10^{-10}$ cm^3 molecules^{-1} s^{-1} and $K_{13} = 8.9 \pm 2.2$.

The study of reaction 12 in its reverse direction allowed a more reliable determination of its equilibrium constant largely as a result of the somewhat slower rate of clustering of H_2CN^+ with HCN in the H_2 carrier gas. The values of k_{-12}/k_{12}, determined from a fit to the H_2COH^+ decay, and K_{-12}, determined from the H_2CN^+/H_2COH^+ ratio plot, were found to be in agreement within experimental error in three experiments in which P had values from 0.363 to 0.370 Torr and the flow of H_2CO had values in the range 4.72–8.1 × 10^{16} molecules s^{-1}. The $H_2COH^+ \cdot H_2CO$ cluster ion present in the flowing H_2CO–H_2 plasma was observed to react with HCN ($k \gtrsim 1 \times 10^{-10}$ cm^3 molecule^{-1} s^{-1}) in a manner which can be represented by the solvated proton-transfer reaction

[14] $H_2COH^+ \cdot H_2CO + HCN \rightarrow H_2CN^+ \cdot H_2CO + H_2CO$

The $H_2CN^+ \cdot H_2CO/H_2COH^+ \cdot H_2CO$ ratio plots indicated that equilibrium was established for this reaction at all flows of HCN and provided a value for $K_{14} = 1.6 \pm 0.6$. A ratio plot analysis of the further reaction of $H_2CN^+ \cdot H_2CO$ with HCN provided three additional determinations of $K_{13} = 8.6 \pm 3.0$ with the equilibrium state now being approached from the reverse direction.

Discussion

Equilibrium Constant Measurements

Confidence in the assertion that the equilibrium constants measured in this study represent true equilibrium is provided by the following observations, each of which is required for equilibria of elementary reactions such as those investigated in this study (7, 9, 15):

(*i*) The agreement between the ratios of rate constants determined from fits to the primary ion decays (which are independent of mass discrimination in the sampling system) and the equilibrium constants determined from the measured equilibrium ion concentrations (corrected for mass discrimination).

(*ii*) The constancy of the measured ratios of rate constants and equilibrium constants over the range in reaction time, neutral concentrations and total pressure adopted in these experiments. In the case of reaction 5, constancy was also observed over the range of electron and ion densities achieved by the addition of SF_6.

(*iii*) The independence of the measured ratios of rate constants and equilibrium constants on the direction of approach to equilibrium (in the case of reactions 9, 10, and 12).

(*iv*) The internal consistency between single-step and multi-step measurements. The equilibrium constant of $(5.8 \pm 1.3) \times 10^2$ determined from a direct study of the H_3O^+/H_3S^+ system agrees within experimental error with the value of $(7.8 \pm 2.7) \times 10^2$ determined indirectly from a study of the H_3O^+/H_2CN^+ and H_3S^+/H_2CN^+ systems. Also the value of 5.1 ± 0.6 for the equilibrium constant of the H_3S^+/H_2CN^+ system compares favourably with the value of 6.3 ± 3.0 which can be derived from the equilibrium constants determined for the H_3S^+/H_2COH^+ and H_2CN^+/H_2COH^+ systems.

A number of reported equilibrium constant measurements performed with a variety of experimental techniques are available for comparison, particularly in the case of reaction 5. These are summarized in Table 3. The deuterium analogue of reaction 5:

[15] $D_3O^+ + D_2S \rightleftarrows D_3S^+ + D_2O$

was investigated by Chong *et al.* (16) in electron impact ion source mass spectrometer experiments involving intensity measurements of D_3O^+ and D_3S^+ in mixtures of D_2O and D_2S in various known proportions at total pressures in the range 0.339–0.680 Torr. Chong *et al.* (16) reported a value for the equilibrium constant of 14.4 ± 1.9 at an ion source temperature of 340 ± 5 K. Hopkins and Bone (17) approached the equilibrium state for [5] in the reverse direction in a photoionization source in mixtures of pure H_2O and H_2S at total pressures ≤ 1.22 Torr and temperatures of 296, 355, and 426 K at which somewhat lower values of 6.7, 2.8, and 1.6, respectively, were obtained for the apparent equilibrium constant. Yamdagni and Kebarle (3) have recently investigated this equilibrium at higher temperatures in the range 570 to 660 K at total pressures in the range 0.5–4 Torr in a pulsed electron-beam ion source. High purity methane was used as the carrier gas in these latter experiments. Moet-Ner and Field (18) have also examined this equilibrium in a pulsed electron-beam ion source in a four-component mixture of 3% H_2O + 1% H_2S + 1% CS_2 in CH_4. In

TABLE 3. Measured equilibrium constants

Reaction	K	T/K	Method[a]
$D_3O^+ + D_2S \rightleftharpoons D_3S^+ + D_2O$	14.4 ± 1.9	340 ± 5	IS
$H_3O^+ + H_2S \rightleftharpoons H_3S^+ + H_2O$	6.7	296	IS–PI
	2.8	355	
	1.6	426	
	~ 10 to ~ 20	570 to 660	HPIS(YK)
	~ 30 to ~ 100	480 to 580	HPIS(MF)
	$(4.4 \pm 0.5) \times 10^2$[b]	303	ICR
	$(5.8 \pm 1.3) \times 10^2$	296 ± 2	FA
$H_3O^+ + HCN \rightleftharpoons H_2CN^+ + H_2O$	$(4.0 \pm 0.9) \times 10^3$	296 ± 2	FA
$H_3S^+ + HCN \rightleftharpoons H_2CN^+ + H_2S$	2.8 ± 0.3	303	ICR
	5.1 ± 0.6	296 ± 2	FA
$H_3S^+ + H_2CO \rightleftharpoons H_2COH^+ + H_2S$	6.2 ± 0.8	303	ICR
	10.0 ± 2.9	296 ± 2	FA
$H_2CN^+ + H_2CO \rightleftharpoons H_2COH^+ + HCN$	2.3 ± 0.3	303	ICR
	1.6 ± 0.3	296 ± 2	FA

[a] IS, electron beam ion source mass spectrometer (16); IS-PI, photoionization source mass spectrometer (17); HPIS, pulsed electron beam high-pressure ion source mass spectrometer (3, 18); ICR, pulsed ion cyclotron resonance (4); FA, flowing afterglow, this work.

[b] Determined indirectly via proton transfer to CF_3CH_2OH but borne out by one direct measurement (see text).

these experiments the temperature was varied between 480 and 580 K at total pressures in the range 0.7–2.5 Torr. Recent pulsed ion cyclotron resonance measurements (4) of the equilibrium state at 303 K for the reactions

[16] $H_3O^+ + CF_3CH_2OH \rightleftharpoons CF_3CH_2OH_2^+ + H_2O$

[17] $CF_3CH_2OH_2^+ + H_2S \rightleftharpoons H_3S^+ + CF_3CH_2OH$

also provide a value for $K_5 = K_{16}K_{17} = (4.4 \pm 0.5) \times 10^2$ which was borne out by one direct measurement of K_5. These measurements were taken at a total pressure of $\sim 10^{-6}$ Torr in the absence of a carrier gas. The flowing afterglow measurements reported here were carried out at 296 ± 2 K in the presence of a large excess of either H_2 or He at total pressures in the range 0.290–0.65 Torr. The results of all six groups of investigators are compared in the Van't Hoff plot shown in Fig. 5. Reasonable agreement is apparent only between the extrapolated high-pressure ion source results of Yamdagni and Kebarle (3), the ion cyclotron resonance measurement at 303 K and the flowing afterglow result reported here. The higher values and temperature dependence of the equilibrium constant implied by the measurements of Moet-Ner and Field (18) lead to a difference of almost an order of magnitude at room temperature. The values of the equilibrium constants reported by Chong *et al.* (16) and Hopkins and Bone (17) are both lower by more than one order of magnitude from the corresponding extrapolated values. In the case of reactions 9, 10, and 12 further comparisons can be made between the results obtained with the ion cyclotron resonance and flowing afterglow techniques. It is apparent from the values given in Table 3 that the equilibrium constants determined with these two techniques for these three reactions disagree within the quoted experimental uncertainties, albeit never by more than a factor of 2.

There are several possible origins for the discrepancies between the various types of measurements. Differences may arise from uncertainties associated with the detection and measurement of ion signals and the measurement of neutral concentrations and temperature. The extent to which such uncertainties contribute to the observed differences could not be ascertained since an adequate assessment of the overall accuracy of the measurements was not always reported. Discrepancies may also arise from differences in conditions prevailing in the actual reaction regions of the various techniques, especially as regards the presence of ambient electric fields, the magnitudes of the temperatures as well as the partial and total pressures and the presence of a carrier gas. The influence of an ambient electric field on equilibrium constant measurements has recently been carefully investigated by Meisels *et al.* (8) particularly in conjunction with such measurements as they are carried out by high-pressure ion source mass spectrometry of the type employed by Chong *et al.* (16). In their systematic study of the equilibrium

[18] $CO_2H^+ + CH_4 \rightleftharpoons CH_5^+ + CO_2$

these authors have observed a strong variation of the value of the equilibrium constant with field strength: for this exothermic reaction the equilibrium constant was observed to decrease substantially as the strength of the ambient field increased, viz. as the average ion energies were shifted upward and the ion velocity distributions lost Maxwell–Boltzmann character. On

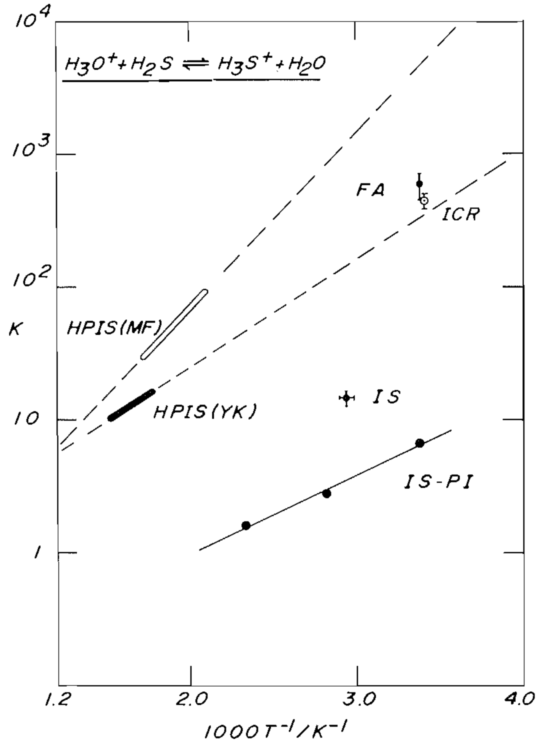

FIG. 5. Van't Hoff plot showing a comparison of the apparent equilibrium constants measured for the reaction $H_3O^+ + H_2S \rightleftharpoons H_3S^+ + H_2O$ with a variety of experimental techniques: IS, electron beam ion source mass spectrometer (16); IS–PI, photo-ionization source mass spectrometer (17); HPIS, pulsed electron beam high-pressure ion source mass spectrometer (3, 18); ICR, pulsed ion cyclotron resonance (4); and FA, flowing afterglow, this work.

the basis of these observations, Meisels *et al.* (8) drew attention to the systematic error that can generally be introduced into equilibrium constant measurements with techniques which employ external fields unless the field strength approaches zero. A second complication is readily apparent from the observations reported by Hopkins and Bone (17) in their study of reaction 5 in its reverse direction. At the temperatures, partial pressures of H_2O and total pressures employed in their experiments, complications were introduced by the clustering of H_3O^+ to higher hydrates, an extraneous sink for H_3O^+ which must be properly taken into account in a complete data analysis. Apparently the rate of clustering of H_3O^+ in these experiments was sufficiently high to prevent the establishment of equilibrium between H_3O^+ and H_3S^+ at all convenient operating conditions. Not being able to determine equilibrium constants directly from a measured H_3O^+ ion signal ratio, these authors were led instead to analyze their data kinetically in terms of a steady state assumption. While the partial pressures of H_2O employed by Chong *et al.* (16) were similar to those used in the photoionization source experiments of Hopkins and Bone (17), those used in the flowing afterglow experiments, the ion cyclotron resonance experiments and the ion source experiments of Yamdagni and Kebarle (3) were many orders of magnitude lower. In the latter two sets of experiments the tendency of H_3O^+ to cluster was reduced still further by the lower total pressures and higher prevailing temperatures, respectively. We have recently considered in detail the constraints introduced into equilibrium constant determinations under flowing afterglow conditions by the occurrence of clustering reactions, indeed of competing reactions generally (14, 15). It was evident from these considerations that a judicious choice of partial pressures of the neutral reagents and the direction of approach to equilibrium is often required to ensure a successful determination of an equilibrium constant. A similar analysis has since been reported by ion cyclotron resonance practitioners (19) who have come to similar conclusions. Finally, only in the high-pressure ion source measurements and the flowing afterglow measurements reported here was it common practice to add a carrier gas in large excess. A carrier gas is normally required to allow both the reactants and products to establish thermal equilibrium with their common surroundings prior to reaction. The uncertainties introduced by the failure to use a carrier gas will be determined in part by the extent to which the product ions are initially formed in disequilibrium and can therefore be expected to be reaction specific. The extent to which the low values of equilibrium constant for [5] obtained in the experiments by Chong *et al.* (16) and Hopkins and Bone (17) which were carried out in pure H_2O/H_2S (D_2O/D_2S) mixtures and the differences between the ion cyclotron resonance and flowing afterglow results for reactions 5, 9, 10, and 12 can be accounted for in this way is uncertain.

Thermochemistry

The changes in standard free energy derived from the equilibrium constant measurements for the five unsolvated proton-transfer reactions and the two solvated proton-transfer reactions investigated in this study are summarized in Table 4. Changes in standard entropy were estimated from changes in molecular rotational symmetry numbers; viz, it was assumed that $\Delta S^0 \approx \Delta S^0{}_{\mathrm{rot}}$ (3, 4). Such a treatment has recently been found to be valid to within ±1.5 cal mol^{-1} deg^{-1} for a large number and variety of proton-transfer reactions (4). In the determination of the rotational symmetry numbers of the ions, account has been taken of what is known from calculations about their geometry (20, 21). The use of

TABLE 4. Changes in the standard free energy (kcal mol^{-1}), standard entropy (cal mol^{-1} deg^{-1}), and standard enthalpy (kcal mol^{-1}) at 298 K

Reaction	$-\Delta G^0{}_{298}{}^a$	$\Delta S^0{}_{298}{}^b$	$-\Delta H^0{}_{298}{}^c$
$H_3O^+ + H_2S \rightleftharpoons H_3S^+ + H_2O$	3.8±0.2	0 ±1.5	3.8±0.6
$H_3O^+ + HCN \rightleftharpoons H_2CN^+ + H_2O$	4.9±0.1	0.8±1.5	4.7±0.5
$H_3S^+ + HCN \rightleftharpoons H_2CN^+ + H_2S$	1.0±0.1	0.8±1.5	0.7±0.5
$H_3S^+ + H_2CO \rightleftharpoons H_2COH^+ + H_2S$	1.4±0.2	2.2±1.5	0.7±0.6
$H_2CN^+ + H_2CO \rightleftharpoons H_2COH^+ + HCN$	0.3±0.1	1.4±1.5	−0.1±0.5
$H_2CN^+{\cdot}HCN + H_2CO \rightleftharpoons H_2COH^+{\cdot}HCN + HCN$	1.3±0.2		
$H_2COH^+{\cdot}H_2CO + HCN \rightleftharpoons H_2CN^+{\cdot}H_2CO + H_2CO$	0.3±0.3		

[a] Calculated from the measured equilibrium constants.
[b] Entropy change due to change in rotational symmetry number (3, 4).
[c] Determined with the relationship $\Delta H^0 = \Delta G^0 + T\Delta S^0$.

entropies of isoelectronic species (given in parentheses) for the ions H_3O^+ (NH_3), H_3S^+ (PH_3), and H_2CN^+ (C_2H_2) provides values for $\Delta S^0{}_{298}$ of 0 ± 0.5, −1.1 ± 1.0, and −1.2 ± 1.0 cal mol^{-1} deg^{-1} for reactions 5, 6, and 9, respectively, when the entropies are taken from the JANAF tables (22). The agreement with the results obtained from the calculations using symmetry numbers is good in the case of reaction 5 but poor for the latter two reactions since the isoelectronic arguments fail to take into account the difference in the rotational symmetry numbers of H_2CN^+ ($H{-}C{\equiv}\overset{+}{N}{-}H$) and C_2H_2. Previous direct experimental determinations of standard entropy changes are available only for reaction 5 and the reaction

[19] $$H_3O^+ + H_2CO \rightleftharpoons H_2COH^+ + H_2O$$

Yamdagni and Kebarle (3) obtained a value of −1.0 ± 0.4 cal mol^{-1} deg^{-1} for ΔS^0 of reaction 5 but these authors were quick to point out that this value is not supported by what is known about the geometrics of H_3O^+ and H_3S^+. Allowing for possible inaccuracies in their experimental determination of ΔS^0, they preferred the value of 0 cal mol^{-1} deg^{-1} arrived at from the isoelectronic and symmetry considerations just mentioned. The value of −5.5 ± 0.2 cal mol^{-1} deg^{-1} derived by Hopkins and Bone (17) from their Van't Hoff plot is clearly unreasonable, while the value of −2.2 ± 1.0 cal mol^{-1} deg^{-1} reported by Moet-Ner and Field (18) appears to be too high. Reaction 19 has been investigated in a variable-temperature flowing afterglow by Fehsenfeld and co-workers (23) who obtained a standard entropy change at a mean temperature of 470 K of 2.2 ± 3.0 cal mol^{-1} deg^{-1} for this reaction which agrees remarkedly well with the sum of the standard entropy changes derived for reactions 5 and 10 from the rotational symmetry arguments.

The value of −3.8 ± 0.6 kcal mol^{-1} for $\Delta H^0{}_{298}$ determined here for reaction 5 may be compared with those which have derived from the Van't Hoff plots shown in Fig. 5: −3.7 ± 0.3 kcal mol^{-1} (3), −2.9 ± kcal mol^{-1} (17), and −5.0 ± 0.4 kcal mol^{-1} (18). Good agreement is apparent only with the results of Yamdagni and Kebarle (3). A comparison may also be made with the value for $\Delta H^0{}_{298}$ which can be derived indirectly from the standard enthalpy changes determined previously by pulsed high-pressure ion source mass spectrometer measurements of the temperature dependence of the equilibrium constants for the reactions [20]–[22]:

[20] $$H_3O^+ + H_2O \rightleftharpoons H_3O^+{\cdot}H_2O$$

[21] $$H_3O^+{\cdot}H_2O + H_2S \rightleftharpoons H_3S^+{\cdot}H_2O + H_2O$$

[22] $$H_3S^+{\cdot}H_2O \rightleftharpoons H_3S^+ + H_2O$$

[5] $$H_3O^+ + H_2S \rightleftharpoons H_3S^+ + H_2O$$

Cunningham *et al.* (24) report a value of −31.6 ± 1 kcal mol^{-1} for ΔH^0 of reaction 20. The very recent measurements of Moet-Ner and Field (25) yielded $\Delta H^0 = -33.0 \pm 1.5$ kcal mol^{-1} for this reaction. These two values combine to yield a weighted mean of −32.1 kcal mol^{-1} with a standard error of ±0.8 kcal mol^{-1} (12). Hiraoka and Kebarle (26) report a value of +6.7 ± 1 kcal mol^{-1} for ΔH^0 of reaction 21 while Moet-Ner and Field (25) obtained a value of +17 ± 1.5 kcal mol^{-1} for ΔH^0 of reaction 22. When these values are adopted, the analysis of the thermodynamic cycle represented by the above four reactions provides a value of −8.4 ± 3.3 kcal mol^{-1} for $\Delta H^0{}_{298}$ of reaction 5 which is considerably higher than the values obtained from the direct measurements of the equilibrium constant for [5]. We are unable to assign the exact origin of this large discrepancy. It appears likely, however, that it reflects a serious shortcoming, presumably of the type discussed in the previous section, in one or more of the equilibrium constant measurements for reactions 20–22. The variable-temperature flowing afterglow measurements for [19] provided a value for $\Delta H^0{}_{470} = -5.2 \pm 0.8$ kcal mol^{-1} (23) which agrees, within experimental error, with the value for

TABLE 5. Summary of proton affinities and heats of formation (kcal mol^{-1}) at 298 K derived from the flowing afterglow equilibrium constant measurements

X	ΔH^0			ΔH^0 (XH^+ to CH_2O)	PA(X)	$\Delta H_f^0(XH^+)$[a]
HCN				+0.1	171.0±1.7	228.5±3.7
	0.1	0.7				
H_2CO				0	170.9±1.2[b]	170.3±1.1[b]
	0.7					
H_2S			4.7	−0.7	170.2±1.8	192.1±2.0
	3.8					
H_2O				−4.5	166.4±2.4	143.0±2.4

[a] $\Delta H_f^0(XH^+) = \Delta H_f^0(X) + \Delta H_f^0(H^+) - PA(X)$. Values for $\Delta H_f^0(X)$ and $\Delta H_f^0(H^+)$ were taken from the JANAF tables (22).

[b] Reference value, see text.

$\Delta H^0{}_{298} = -4.5 \pm 1.1$ kcal mol^{-1} derived from the standard enthalpy changes determined in this study for reactions 5 and 10.

When combined with those of the corresponding unsolvated proton-transfer reactions, the standard free energy changes derived from the equilibrium constant measurements for the solvated proton transfer reactions provide information about the standard free energies of dissociation of the solvated ions. In the case of 'heterogeneous' solvated ions, XH^+Y in which the proton is shared between two different molecules, we can distinguish between two paths of dissociation and therefore two free energies of dissociation which are related according to the following thermochemical cycle:

[23]
$$\begin{tikzcd} & XH^+Y \arrow[dl, "D_1"'] & \\ XH^+ + Y \arrow[rr, "3"'] & & YH^+ + X \arrow[ul, "-D_2"'] \end{tikzcd}$$

The standard free energies of dissociation D_1 and D_2 differ by an amount given by the standard free energy change associated with the proton-transfer step *3*. This notion is expressed explicitly by the manner in which we have chosen to write the molecular formula of the solvated ions, viz. we have artificially distinguished between $XH^+{\cdot}Y$ and $YH^+{\cdot}X$. This convention facilitates the comparison of unsolvated and solvated proton transfer and is not meant to imply a difference in structure or energy. It is readily apparent from a comparison of reaction 1 and the generalized solvated proton-transfer reaction

[24] $$XH^+{\cdot}X + Y \rightleftarrows YH^+{\cdot}X + X$$

that the standard free energy change associated with a solvated proton-transfer reaction will differ from that associated with its unsolvated counterpart by the difference in the standard free energies of dissociation of the two solvated ions, viz. $D(XH^+ - X) - D(YH^+ - X)$. Thus a comparison of the values for ΔG^0 determined for reactions 12 and 13 provides a value for the difference in standard free energies of dissociation, $D(H_2COH^+ - HCN) - D(H_2CN^+ - HCN)$, of $+1.0 \pm 0.3$ kcal mol^{-1} whereas such a comparison for reactions 12 and 14 provides a value for $D(H_2CN^+ - H_2CO) - D(H_2COH^+ - H_2CO)$ of $+0.6 \pm 0.4$ kcal mol^{-1}. A value of $+0.3 \pm 0.1$ kcal mol^{-1} is obtained for $D(H_2CN^+ - H_2CO) - D(H_2COH^+ - HCN)$ when ΔG^0 determined for reaction 12 is incorporated into the thermochemical cycle [23]. This result simply reflects the slightly higher basicity (expressed as a free energy) of H_2CO. Finally a thermochemical analysis of the cycle comprising reactions 12–14 provides a value for $D(H_2COH^+ - H_2CO) - D(H_2CN^+ - HCN) = +0.7 \pm 0.5$ kcal mol^{-1}.

Proton Affinities

The standard enthalpy changes determined in this investigation for the reactions of type [1] are presented in Table 5 in the form of a proton affinity 'ladder' together with the corresponding proton affinities and heats of formation of the protonated species. The proton affinity ladder is referenced to the proton affinity of H_2CO which was derived from the photoionization appearance potential of 11.67 ± 0.03 eV for H_2COH^+ from CH_3OH as measured by Refaey and Chupka (2). Adoption of the values for $\Delta H^0{}_{f,0}(H)$ and $\Delta H^0{}_{f,0}(CH_3OH)$ tabulated in the recent compilation by Rosenstock *et al.* (27) leads to a value for $\Delta H^0{}_{f,0}(H_2COH^+) = 172.1 \pm 0.7$ kcal mol^{-1} and for $\Delta H^0{}_{f,298}(H_2COH^+) = 170.3 \pm 1.1$ kcal mol^{-1} when a correction is made for temperature by comparison with similar molecules (2); (we have assigned an uncertainty of ±20% to this correction). A value for $PA_{298}(CH_2O) = 170.9 \pm 1.2$ kcal mol^{-1} can then be derived using $\Delta H^0{}_{f,298}(CH_2O) = -25.95 \pm 0.11$ kcal mol^{-1} as determined by Fletcher and Pilcher (28) and the $\Delta H^0{}_{f,298}(H^+)$ in the JANAF tables (22).

Our values for $PA_{298}(HCN)$ and $PA_{298}(H_2S)$ agree within experimental error with the value 170 ± 3 kcal mol^{-1} derived for the proton affinity of these two molecules by Haney and Franklin (29). The value of $PA(H_2S)$ was determined by these latter authors

TABLE 6. Summary of rate constants (10^{-9} cm^3 molecule^{-1} s^{-1}) at 296 ± 2 K

Reaction	k_{exptl}	k_{capture}	$k_{\mathrm{exptl}}/k_{\mathrm{capture}}$
$H_3O^+ + H_2S \rightarrow H_3S^+ + H_2O$	1.9±0.4	1.65	1.1 ±0.2
$H_3O^+ + HCN \rightarrow H_2CN^+ + H_2O$	3.5±0.7	3.20	1.1 ±0.2
$H_3S^+ + HCN \rightarrow H_2CN^+ + H_2S$	1.5±0.4	2.74	0.56±0.14
$H_3S^+ + H_2CO \rightarrow H_2COH^+ + H_2S$	2.2±0.6	2.23	1.0 ±0.3
$H_2CN^+ + H_2CO \rightarrow H_2COH^+ + HCN$	≥1.6	2.35	≥0.69

[a] The mean value together with the estimated accuracy of the measurements.

[b] Calculated using the $\overline{\cos \theta}$ model of the Average-Dipole-Orientation theory (32). $C = 0.144$, 0.252, and 0.234 for the reactions with H_2S, HCN, and H_2CO respectively; $\alpha(HCN) = 2.59$ Å^3 (33), $\alpha(H_2S) = 3.64$ Å^3 (34), $\alpha(H_2CO) = 2.81$ Å^3 (35); $\mu_D(HCN) = 2.98$ D, $\mu_D(H_2S) = 0.97$ D, $\mu_D(H_2CO) = 2.33$ D (36).

from appearance potential measurements for electron impact fragmentation of ethanethiol and dimethylsulfide while PA(HCN) was tied to PA(H_2S) through the observation of proton transfer between these two molecules. Our value for $PA_{298}(H_2O)$ agrees within experimental error with the 'best' value of 165 ± 3 kcal mol^{-1} adopted by Long and Munson (5) in their consideration of the proton affinities of oxygenated compounds but is somewhat lower than the values of 168.9 ± 2 kcal mol^{-1} derived recently by Yamdagni and Kebarle (3) and 170.3 ± 2 kcal mol^{-1} preferred by Wolf *et al.* (4).

One problem generally encountered in equilibrium studies directed towards the determination of an accurate absolute value of the proton affinity of a specific molecule has been to incorporate that molecule into a proton affinity ladder in close proximity to a reference molecule whose absolute proton affinity has been accurately established with other methods. The uncertainty in the proton affinity of the desired molecule is then determined both by the uncertainty in the absolute standard and the uncertainty which accumulates according to the number of equilibrium steps between that molecule and the reference molecule. In the case of single temperature measurements this uncertainty will include that associated with the estimation of ΔS^0. As regards the determination of $PA_{298}(H_2O)$, we are fortunate in this study to have available as a reference a relatively accurate value for $PA_{298}(CH_2O)$ with CH_2O being only two equilibrium steps removed from H_2O. In the equilibrium studies of Yamdagni and Kebarle (3) isobutene was chosen as the reference molecule. It was only three equilibrium steps removed from NH_3, the molecule whose proton affinity was desired, but at least ten equilibrium steps removed from H_2O. For each step between isobutene and H_2O, including the H_2S/H_2O equilibrium for which a value for ΔH^0 had actually been derived from a Van't Hoff plot, $\Delta G^0{}_{600}$ was assumed to be equal to $\Delta H^0{}_{298}$. These considerations, including the uncertainty in PA_{298} (isobutene) which we estimate to be $\gtrsim 4$ kcal mol^{-1} (largely due to the uncertainty in ΔH_f(*tert*-butyl radical) (30)), are probably sufficient to account for the apparent discrepancy between the values for $PA(H_2O)$ determined by these authors and in the present study. The origin of the value for $PA(H_2O)$ of 170.3 ± 2 kcal mol^{-1} was not discussed in the paper by Wolf *et al.* (4). It is due to appear in a separate publication by these authors.

Rate Constant Measurements

The unsolvated proton-transfer reactions investigated in this study were all observed to proceed rapidly ($k \gtrsim 1 \times 10^{-9}$ cm^3 molecule^{-1} s^{-1}) in the forward (exoergic) direction, in accord with expectations based on our growing experience for such reactions (31). The measured rate constants for the individual reactions are summarized in Table 6. They appear not to have been determined previously by other workers although Chong *et al.* (16) have reported a rate constant in the range 0.8–1.9 × 10^{-9} cm^3 molecule^{-1} s^{-1} for reaction 15, the deuterium analogue of reaction 5. Table 6 also includes a comparison of the measured reaction rate constants with collision rate constants calculated using the Average-Dipole-Orientation theory (32). The consonance between these two sets of values is again not surprising (31).

The much larger range in values observed for the rate constants of the solvated proton-transfer reactions (see Table 2) is most readily understood in terms of overall reaction energetics. For several of these reactions the difference in the standard free energies of dissociation of the two solvated ions appears to be sufficient to cause a change in the sign of the standard free energy change associated with the unsolvated counterpart. This is not surprising in view of the low exoergicity, $\Delta G^0{}_{298} \lesssim 5$ kcal mol^{-1}, generally exhibited by the corresponding unsolvated reactions. In the case of reactions 12–14 our equilibrium constant measurements indicate that the solvation of H_2CN^+ by one HCN molecule actually increases the exoergicity for proton transfer by 1.0 kcal mol^{-1} while solvation by one H_2CO molecule decreases the exoergicity from −0.3 to +0.3 kcal mol^{-1}. These observations are borne out by the corresponding rate constant measurements which indicate that $H_2CN^+ \cdot HCN$ still undergoes proton transfer with H_2CO with a relatively large rate constant, albeit slightly lower than that for its unsolvated counterpart, and that $H_2COH^+ \cdot H_2CO$ reacts rapidly with HCN to produce $H_2CN^+ \cdot H_2CO$. The rate constant for proton transfer between H_3O^+ and HCN is decreased significantly upon the solvation of H_3O^+ with one H_2O molecule. The low value for k_7 of 1×10^{-10} cm^3 molecule^{-1} s^{-1} suggests that this solvated reaction may in fact be slightly endoergic with $D(H_3O^+ - H_2O) - D(H_2CN^+ - H_2O) \approx 6$ kcal mol^{-1}. There is much less doubt about the overall energetics of the reaction of unsolvated and solvated H_3O^+ with H_2S. The recent measurements of Hiraoka and Kebarle (26) indicate standard free energy changes at 300 K for the reactions

$$[25] \qquad H_3O^+ \cdot H_2O + H_2S \rightleftarrows H_3S^+ \cdot H_2O + H_2O$$

$$[26] \qquad H_3O^+ \cdot 2H_2O + H_2S \rightleftarrows H_3S^+ \cdot 2H_2O + H_2O$$

of $+7.1 \pm 0.5$ and $+6.3 \pm 0.6$ kcal mol^{-1}, respectively, which correspond to a decrease of ~ 10 kcal mol^{-1} in ΔG^0 upon hydration of H_3O^+. Our observations indicate a concomitant decrease in the value of k by more than 10^3 from 1.9×10^{-9} to $\lesssim 1 \times 10^{-12}$ cm^3 molecule^{-1} s^{-1}. Finally the drop in the value of k from 3×10^{-10} to $\lesssim 1 \times 10^{-12}$ cm^3 molecule s^{-1} observed for the endoergic proton transfer from H_2CN^+ to H_2S suggests an even larger endoergicity for the $H_2CN^+ \cdot HCN$ reaction with $D(H_2CN^+ - HCN) > D(H_3S^+ - HCN)$.

Acknowledgements

We thank Dr. Fehsenfeld for a preprint of ref. 23 and Professor R. W. Taft for a preprint of ref. 4 and for providing us with the values of the equilibrium constants measured with the pulsed ion cyclotron resonance technique. We are grateful to the National Research Council of Canada and the Sloan Foundation for financial support.

1. P. Ausloos (*Editor*). Interactions between ions and molecules. Plenum Press, New York, NY. 1975.
2. K. M. A. Refaey and W. A. Chupka. J. Chem. Phys. **48**, 5205 (1968).
3. R. Yamdagni and P. Kebarle. J. Am. Chem. Soc. **98**, 1320 (1976).
4. J. F. Wolf, R. H. Staley, I. Koppel, M. Taagepera, R. T. McIver, J. L. Beauchamp, and R. W. Taft. J. Am. Chem. Soc. In press.
5. J. Long and B. Munson. J. Am. Chem. Soc. **95**, 2427 (1973).
6. R. H. Staley and J. L. Beauchamp. J. Chem. Phys. **62**, 1998 (1975).
7. D. Betowski, G. Mackay, J. Payzant, and D. Bohme. Can. J. Chem. **53**, 2365 (1975).
8. G. G. Meisels, R. K. Mitchum, and J. P. Freeman. J. Phys. Chem. **80**, 2845 (1976).
9. D. K. Bohme, R. S. Hemsworth, H. W. Rundle, and H. I. Schiff. J. Chem. Phys. **58**, 3504 (1973).
10. G. Brauer (*Editor*). Handbook of preparative inorganic chemistry. Academic Press, New York, NY. 1965.
11. R. Spence and W. Wild. J. Chem. Soc. 338 (1935).
12. N. C. Barford. Experimental measurements: precision, error and truth. Addison-Wesley, London. 1967.
13. G. I. Mackay, L. D. Betowski, J. D. Payzant, H. I. Schiff, and D. K. Bohme. J. Phys. Chem. **80**, 2919 (1976).
14. G. I. Mackay, R. S. Hemsworth, and D. K. Bohme. Can. J. Chem. **54**, 1624 (1976).
15. D. K. Bohme and G. I. Mackay. 24th Am. Conf. Mass Spectrom. Allied Topics, San Diego, California, May, 1976.
16. S. L. Chong, R. A. Myers, and J. L. Franklin. J. Chem. Phys. **56**, 2427 (1972).
17. J. M. Hopkins and L. I. Bone. J. Chem. Phys. **58**, 1473 (1973).
18. M. Meot-Ner and F. H. Field. J. Chem. Phys. **66**, 4527 (1977).
19. W. R. Davidson, M. T. Bowers, T. Su, and D. H. Aue. Intern. J. Mass Spectrom. Ion Phys. **24**, 83 (1977).
20. A. C. Hopkinson. Prog. Theor. Org. Chem. **2**, 194, (1977).
21. A. C. Hopkinson, N. K. Holbrook, K. Yates, and I. G. Csizmadia. J. Chem. Phys. **49**, 3596 (1968).
22. JANAF Thermochemical Tables. 2nd ed. Natl. Stand. Ref. Data Serv. Natl. Bur. Stand. **37** (1971).
23. F. C. Fehsenfeld, I. Dotan, D. L. Albritton, C. J. Howard, and E. E. Ferguson. J. Geophys. Res. In press.
24. A. J. Cunningham, J. D. Payzant, and P. Kebarle. J. Am. Chem. Soc. **94**, 7627 (1972).
25. M. Meot-Ner and F. H. Field. J. Am. Chem. Soc. **99**, 998 (1977).
26. K. Hiraoka and P. Kebarle. Can. J. Chem. **55**, 24 (1977).
27. H. M. Rosenstock, K. Draxl, B. W. Steiner, and J. T. Herron. J. Phys. Chem. Ref. Data, **6** (1977).
28. R. A. Fletcher and G. Pilcher. Trans. Faraday Soc. **65**, 113 (1968).
29. M. A. Haney and J. L. Franklin. J. Chem. Phys. **50**, 2028 (1968).
30. W. Tsang. J. Phys. Chem. **76**, 143 (1972).
31. D. K. Bohme. *In* Interactions between ions and molecules. *Edited by* P. Ausloos. Plenum Press, New York, NY. 1975.
32. L. Bass, T. Su, W. J. Chesnavich, and M. T. Bowers. Chem. Phys. Lett. **34**, 119 (1975).
33. J. O. Hirschfelder, G. F. Curtiss, and R. B. Bird. Molecular theory of gases and liquids. John Wiley and Sons, New York, NY. 1954.
34. E. R. Lippincott and J. M. Stutman. J. Phys. **31**, 1619 (1959).
35. E. W. Rothe and R. B. Bernstein. J. Chem. Phys. **31**, 1619 (1959).
36. R. D. Nelson, D. R. Lide, and A. A. Marjott. Natl. Stand. Ref. Data Ser. Natl. Bur. Stand. **10** (1966).